Transparent ternary alloy counter electrodes for high-efficiency bifacial dye-sensitized solar cells

Tianshu Liu[a], Yuanyuan Zhao[a], Jialong Duan[a], Benlin He[a], Jingjing Zheng[b], Qunwei Tang[c,d,*]

[a] School of Materials Science and Engineering, Ocean University of China, Qingdao 266100, PR China
[b] Department of Chemical Engineering and Safety, Binzhou University, Binzhou 256603, PR China
[c] Institute of New Energy Technology, College of Information Science and Technology, Jinan University, Guangzhou 510632, PR China
[d] Joint Laboratory for Deep Blue Fishery Engineering, Qingdao National Laboratory for Marine Science and Technology, Qingdao 266237, PR China

ARTICLE INFO

ABSTRACT

Bifacial dye-sensitized solar cells (DSSCs) are regarded as promising photovoltaics to harvest solar energy from both front and rear sides because of their significantly increased total power outputs. Transparent counter electrodes (CEs) with cost-effectiveness and high electrocatalytic activity are crucial to make these high-performance bifacial devices. Herein, a category of transparent CEs from ternary alloys [$(CoM)_{0.85}Se$, M = Ni, Ru, Fe] are synthesized by a mild solution method. Upon careful optimization on optical behaviors, electrocatalytic activity and photovoltaic performances, the bifacial DSSCs with $(CoNi)_{0.85}Se$, $(CoRu)_{0.85}Se$, $(CoFe)_{0.85}Se$ CEs achieve front power conversion efficiencies of 9.14%, 8.09%, 7.58% and rear efficiencies of 3.86%, 3.31%, 3.51% in comparison with 6.72% and 3.16% for state-of-the-art Pt CE based solar cell, respectively. Moreover, these bifacial DSSCs devices display high multiple on/off capability and relatively good stability.

1. Introduction

Solar energy is considered as a viable solution to environmental and energy issues due to the clean and inexhaustible advantages. Photovoltaic technology is promising in directly converting solar energy into electricity through complicated photoelectric processes. Since the first prototype of dye-sensitized solar cell (DSSC) developed by O'Regan and Grätzel (1991); Jin et al., 2017), it has attracted numerous attention and industrial interests because of its simple fabrication, environmental friendliness and low cost. As a crucial part of a classic DSSC device, the counter electrode (CE) plays an important role in collecting electrons from external circuit and catalyzing the reduction reaction of $I_3^- + 2e = 3I^-$. Traditionally, platinum (Pt) is a preferred CE material due to high conductivity and electrocatalytic performances toward redox electrolyte. However, the high price of Pt has been an economic burden for the commercialization of DSSCs (Xi et al., 2017). Therefore, it is a prerequisite to develop alternative CEs with cost-effectiveness, high conductivity and good electrocatalytic activity. Till now, the Pt-free CEs from carbonaceous materials (Li et al., 2018; Chen et al., 2016; Gao et al., 2018; Wang et al., 2017), conducting polymers (Hammed et al., 2017; Li et al., 2017a, 2017b) and compounds (Liu et al., 2018) have been successfully made to replace precious Pt electrode, but their long-term stability and catalytic ability are still

unsatisfactory to meet requirements. The rational design of low-cost, highly catalytic and electrolyte-tolerant CEs seems to be urgent for advanced DSSCs.

Despite the maximum efficiency of liquid-junction DSSC has reached to 14% (Kakiage et al., 2015), the inherent limitations of charge transfer remain a significant barrier to cut down the cost of photovoltaic conversion. Bifacial DSSCs are considered as a promising strategy to reduce the cost of power generation owing to its unique ability to convert solar energy into electricity from both front and rear sides (Zhang et al., 2018). In this fashion, exploring highly transparent CEs without bring down their catalytic capacity is a major issue in the design of such bifacial DSSCs (Yang and Tang, 2016). Although graphene (Yang et al., 2015) and conducting polymers (Park et al., 2017) have been employed as transparent CEs, the ability to catalyze the redox electrolyte is limited and their capacity of electron collection from external circuit is poor, impeding the improvement of solar cell efficiency. According to previous reports, transition metal transparent CEs have been demonstrated to be the most appealing substitutes for DSSCs. Especially, ternary compounds exhibit higher redox potential and excellent electrochemical characteristics compared with binary compounds due to synergistic effect (Qian et al., 2016; Chen et al., 2017; Li et al. 2017a, 2017b). Therefore, we demonstrate here the synthesis of transparent CEs from $(CoM)_{0.85}Se$ (M = Ni, Ru, Fe) alloys

---
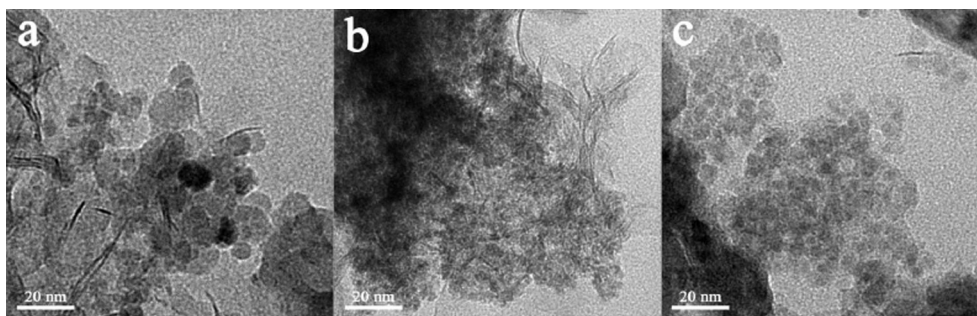
Fig. 1. TEM photographs of (a) $(CoNi)_{0.85}Se$, (b) $(CoRu)_{0.85}Se$, and (c) $(CoFe)_{0.85}Se$ alloys.

by a mild solution method. The resultant $(CoNi)_{0.85}Se$ alloy CE displays higher optical transmittance and catalytic performance, yielding an optimal front efficiency of 9.14% and a rear efficiency of 3.86% in corresponding DSSC device.

2. Experimental

2.1. Synthesis of ternary $(CoM)_{0.85}Se$ (M = Ni, Fe, Ru) alloy CEs

The ternary $(CoM)_{0.85}Se$ (M = Ni, Fe, Ru) alloy CEs were synthesized by a hydrothermal process. Se powders, $CoCl_2 \cdot 6H_2O$ and salts for Ni, Fe or Ru with determined stoichiometries [$(CoNi)_{0.85}Se$: 0.01 g of Se powders and 0.0243 g of $CoCl_2 \cdot 6H_2O$ and 0.0242 g $NiCl_2 \cdot 6H_2O$, $(CoRu)_{0.85}Se$: 0.01 g of Se powders and 0.0244 g of $CoCl_2 \cdot 6H_2O$ and 0.02 g of $RuCl_3 \ 3H_2O$, $(CoFe)_{0.85}Se$: 0.01 g of Se powders and 0.0243 g of $CoCl_2 \cdot 6H_2O$ and 0.0276 g $FeCl_3 \cdot 6H_2O$] were added into 35 mL of deionized water and 2 mL of hydrazine hydrate (85 wt%). After vigorous agitation for 10 min under 600 rpm, the mixture was transferred into a 50 mL Teflon-lined autoclave and then a fluorine-doped tin oxide (FTO) substrate was downwardly immersed into the above solution for the deposition of transparent ternary alloy CE. The standard Pt electrode was purchased from Dalian HeptaChroma SolarTech Co, Ltd.

2.2. Fabrication of DSSCs

The transparent alloy CEs were prepared by a hydrothermal method. In detail, a fluorine-doped tin oxide (FTO) substrate was rinsed with acetone, ethanol and deionized water and then immersed into prepared mixture. After heating for 12 h at 120 °C, the FTO substrates were rinsed with deionized water and dried at 50 °C in air. The sandwiched structure of DSSCs were fabricated comprising of a mesoscopic TiO_2 photoanode, a redox electrolyte having I^-/I_3^- couples and a transparent alloy CE. The TiO_2 colloid was prepared according to the previous report (Wang et al., 2015) and coated by a doctor-blade method. TiO_2 electrode was soaked in 50 mM N719 solution for 24 h. A redox electrolyte consisting of 100 mM of tetraethylammonium iodide, 100 mM of tetramethylammonium iodide, 100 mM of tetrabutylammonium iodide, 100 mM of NaI, 100 mM of KI, 100 mM of LiI, 50 mM of I_2, and 500 mM of 4-*tert*-butyl-pyridine in 50 mL acetonitrile was injected into the interspace between the dye-sensitized TiO_2 photoanode and the CE.

2.3. Electrochemical characterizations

Cyclic voltammetry (CV) experiments were performed on a three-electrode system containing a working electrode of $(CoM)_{0.85}Se$ alloy electrode, a CE of Pt sheet, and a reference electrode of Ag/AgCl. The CV curves were scanned from −0.6 to 1.2 V and back to −0.6 V in a supporting electrolyte of acetonitrile solution consisting of 10 mM of I_2, 50 mM of LiI, 500 mM of $LiClO_4$.

2.4. Photovoltaic measurements

A CHI660E electrochemical workstation was used to test photovoltaic performances of DSSCs. The power conversion efficiency was demonstrated by photocurrent-voltage (*J-V*) characteristic curves using a solar simulator (Newport, Oriel Class A, 91195A) under AM 1.5G simulated solar illumination (100 mW cm^{-2}, calibrated by a standard silicon solar cell). The photovoltaic curves were recorded at room temperature in ambient atmosphere.

2.5. Other characterizations

The properties of alloys were observed by using transmission electron microscopy (TEM, FEI Tecnai G20). Incident photo-current conversion efficiency (IPCE) curves were gained by an IPCE measurement systems with wavelength range of 300–1000 nm. X-ray photoelectric spectroscopy (XPS) profiles were recorded on an ESCALAB 250Xi detector with Al K_α radiation (hv = 1486.6 eV) The optical transmission spectra of the resulting CEs was determined on a UV–visible spectrophotometer.

3. Results and discussion

The transmission electron microscopy (TEM) images of $(CoNi)_{0.85}Se$, $(CoRu)_{0.85}Se$, and $(CoFe)_{0.85}Se$ alloys are shown in Fig. 1. The small particles and lamellar phases can increase the exposure area of alloy CEs to redox electrolyte, providing more ion channels and active sites for the diffusion of ions and reduction of I_3^-. It can be inferred from the result that alloy CEs may exhibit excellent ability in reduction reaction of I_3^-/I^-.

Fig. 2 shows the XPS spectra of alloy CEs and the resultant binding energies of Se 3d, Ni 2p, Co 2p, Ru 3d and Fe 2p. It can be found from Fig. 2b, the binding energy of Se shifts to 54.6 eV compared with standard binding energy of 55.4 eV (Canava et al., 2002; Huo et al., 2016). The Ni, Co elements in $(CoNi)_{0.85}Se$ alloy are in their metallic state, as shown in Fig. 2c, d, and the binding energies of Ni, Co shift to 856.07 eV and 778.35 eV from 857 eV and 778.5 eV, respectively. According to previous literatures, the peak shift is mainly attributed to the alloying of several elements (Shao et al., 2017; Wang et al., 2016), suggesting that $(CoNi)_{0.85}Se$ alloy has been formed by the hydrothermal method (Yang et al., 2016). Similarly, metallic Co, Ru and Fe are also found in $(CoRu)_{0.85}Se$ and $(CoFe)_{0.85}Se$ alloys. The XPS characterization cross-checks the alloying characteristic of transparent ternary CEs. Moreover, a large number of defects and lattice distortion may be produced during alloying process to adsorb I_3^- ions for subsequent catalytic reaction.

The catalytic activity is crucial to assess the performance of a CE. Fig. 3a shows CV curves of different CEs recorded at a scan rate of 50 mV s^{-1}. There are two pairs of oxidation-reduction peaks in each alloy CE based CV curve (Red_1: $I_3^- + 2e = 3I^-$, Ox_1: $3I^- - 2e = I_3^-$; Red_2: $3I_2 + 2e = 2I_3^-$, Ox_2: $2I_3^- - 2e = 3I_2$). The shape and peak position are similar to that of standard Pt electrode, indicating that the